Bend Beam Method for Determining Fracture Properties of Concrete: I. Nonlinear Fracture Mechanics Model

Pusit Lertwattanaruk
Faculty of Architecture and Planning, Thammasat University,
Khlong Luang, Pathumthani, 12121, THAILAND
Tel: (+662) 986-9605, Fax: (+662) 986-9434
E-mail: Lertwatt@tu.ac.th

Abstract

While the linear elastic fracture mechanics (LEFM) concept is not appropriate to describe fracture characteristics of concrete, a nonlinear fracture mechanics model based on the load vs. deflection and load vs. crack-mouth-opening displacement (CMOD) responses of the three-point bend tests on notched beams is proposed. The proposed fracture model is capable of generating the load vs. crack growth curve and the strain energy release rate (G_R) vs. crack growth curve. The conventional fracture parameters such as the fracture energy (G_F), critical effective crack length (a_c) and critical strain energy release rate (G_C) can be obtained as well. In this study, normal concrete and silica fume concrete were prepared as specimens. Through experimental and parametric study, improving the pre-peak fracture behavior of concrete e.g. the critical energy release rate (G_C) does not necessarily enhance the overall fracture behavior. The validity of the proposed fracture model is verified through a comparison of the experimental and analytical results.

1. Introduction

Several fracture mechanics approaches have been proposed to study the fracture behavior of concrete. These promising approaches primarily include the Fictitious Crack Model (FCM) by Hillerborg et al. [1], the Two Parameter Fracture Model (TPFM) by Jenq and Shah [2], and the Size Effect Model (SEM) by Bazant and Kazemi [3]. Each of these models introduces some material fracture properties regardless of the structural geometry and the size. In order to use any of these models in practice, material fracture parameters have to be experimentally evaluated.

Fracture energy (G_F), a material property, is one of the very important parameters used in studying fracture behavior of concrete. It is the amount of energy required to extend a unit crack area through the material. If fracture energy is known then the overall fracture behavior of a structure can be predicted more accurately. The most widely used fracture mechanics model for analyzing concrete structures is the Fictitious Crack Model (FCM). To implement FCM, which requires finite element analysis, both the fracture energy and tensile strength of material need to be determined and incorporated. If these values are not accurately available the analysis for the fracture behavior and other fracture parameters will not be accurate.

Survey of numerous fracture energy tests by using three-point bend tests on notched beams based on the RILEM TC 50-FMC method [4] indicating the load-line deflection measurement is strongly affected by the support conditions. The crack mouth opening displacements on the other hand are not to be affected by the test setups in any way. Based on this fact, Kim [5] found a more reliable method for evaluating the fracture energy of concrete by using the relationship between the load-line deflection and crack-mouth-opening displacement (CMOD).

The Two Parameter Fracture Model (TPFM) proposed the fracture parameters including the critical crack length (a_c), critical stress intensity factor (K_{IC}), critical crack tip

RECEIVED 14 October, 2005
ACCEPTED 15 March, 2006

opening displacement ($CTOD_C$) and critical energy release rate (G_C) as material properties [2]. These parameters are derived based on the linear elastic fracture mechanics (LEFM) concept, which is not suitable for nonlinear behavior of concrete. According to RILEM TC 89-FMT [6], the three-point bend specimen is needed, and the testing procedure also requires an unloading and reloading. To achieve a stable unloading after the peak load, a closed loop testing system is usually required, making the testing method restrictive to most practical engineering testing laboratories.

Several researchers [1,7-9] studied the performance of concrete based on the Fictitious Crack Model (FCM). The FCM model depends heavily on the tensile strength (f_t') and the criterion crack opening displacement (w_c) of material, which are obtained only by the direct tension test, or otherwise, have to be assumed, in order to apply the finite element model to study fracture behavior of concrete. If the value of tensile strength is not accurate, the FCM will not provide the true characteristics of concrete.

In this study based on the three-point bend test on notched beam, the concept of load-line deflection and CMOD relationship is adopted to develop a nonlinear fracture model without requiring the direct tension test and finite element model. The fracture behaviors of concrete provided are crack growth and various fracture properties such as fracture energy, energy release rate and fracture toughness. Also the fracture parameters as outlined in the Two-Parameter Fracture Model i.e. the critical energy release rate (G_C) and critical crack length (a_c) can be obtained without performing the complicated unloading and reloading during test. The proposed model as a result is instrumental for further studies of the influence of cement matrix modification on fracture behavior of concrete.

2. Experimental Program

To study the fracture behavior of concrete, the experimental program was designed to yield the test data required to implement the proposed fracture model. The three-point bend tests on notched beams, designed to eliminate the effects of support crushing, were conducted to obtain the test data comprising of the load-line deflection (LLD), crack-mouth-opening displacement (CMOD) and applied loads. The mechanical properties of concrete were also investigated by performing the uniaxial compression tests. A series of specimens for the control concrete and silica fume concrete with compressive strengths ranging between 41 KPa and 51 KPa were tested.

2.1 Details of Concrete Mix and Materials

Details of the mix proportions of the concrete are presented in Table 1. The control concrete (CC) without any additives and silica fume concrete (SF) were cast. In this study, Portland cement Type I conforming to ASTM C 150 were used. Silica fume with particle size less than 1 μm were used as an additive. Local siliceous sand, passing through sieve No. 4 (opening size 4.75 mm) conforming to ASTM C 33, were used as fine aggregates. Coarse aggregates were crushed limestone of 3/8 inch (9.5 mm) maximum size. Tap water was used throughout the experiment program.

Table 1 Mix proportions of concrete by weight

Materials	Control Concrete (CC)	Silica Fume Concrete (SF)
Cement	1	0.9
Sand	2	2
Coarse Aggregate	3	3
Water	0.5	0.5
Silica Fume	0	0.1

2.2 Uniaxial Compression Test of Concrete

The 75 x 160 mm cylinders were cast in plastic molds and rested in the normal room environment. After 24 hours they were demolded, and then transferred into a 100% humidity room for curing. All cylinders were tested at the age of 56 days. The primary objective of this test is to determine the concrete mechanical properties such as the

compressive strength (f_c'), and the Modulus of Elasticity (E_c), according to ASTM C-39 and ASTM C-469 standards [10].

2.3 Three-Point Bend Test on Notched Beam

The 75 x 57 x 400 mm beams were cast and rested in the normal room environment. After 24 hours they were demolded, and then transferred into a 100% humidity room for curing until one day before testing. Prior to testing the beams were notched using a circular diamond saw. All beams were tested at the age of 56 days. Fig. 1 shows the diagram of the beam test setup and the dimension of the test specimens. Fig. 2 shows the photographs of the three-point bend beam test setup where special arrangement was made to accurately measure the load-line deflection.

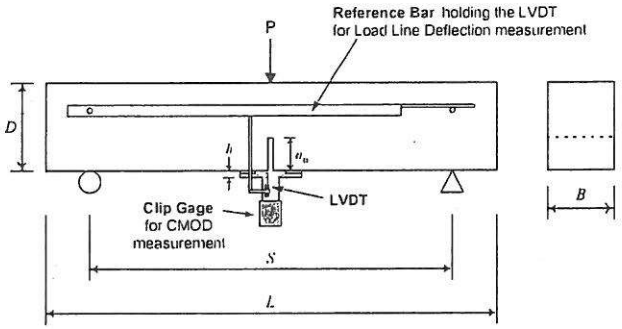

Fig. 1 Three-point-bend beam test setup

L is the specimen length (400 mm); S is the span length (300 mm); D is the beam depth (75 mm); B is the width (75 mm), and a_0 is the initial notch depth (25 mm).

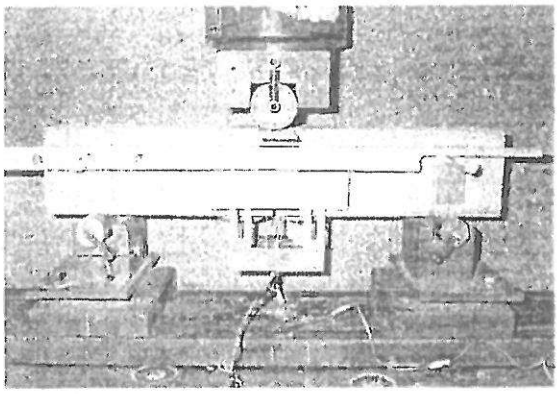

Fig. 2 Photograph of the three-point-bend beam test setup

The main purpose of the three-point-bend beam test is to obtain the load vs. crack-mouth-opening displacement (CMOD) curve and load vs. load-line deflection (LLD) curve, and to study the fracture behavior of concrete by implementing the proposed model.

All beam tests were performed under the CMOD control in an MTS closed-loop testing system at a displacement rate of 5 x 10^{-4} mm/second to produce a controlled failure, allowing all parameters of interest to be measured. The load-line deflection (LLD) was measured off a reference frame using a linear variable differential transformer (LVDT). The measurements of CMOD were done by an MTS clip-on gage. For further study, in order to compare with the Two-Parameter Fracture Model [2], the applied load was unloaded when passed the maximum load at about 95%, and reloaded when the applied load approached zero. It took approximately 45 minutes to an hour to complete the entire test.

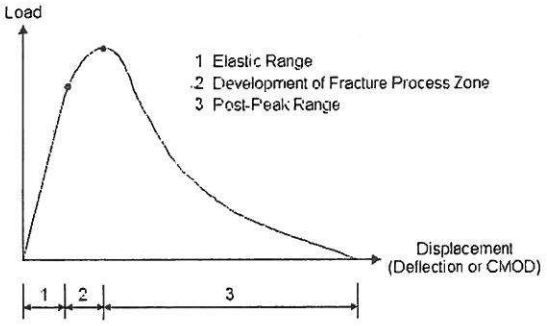

Fig. 3(a) Typical load-displacement response

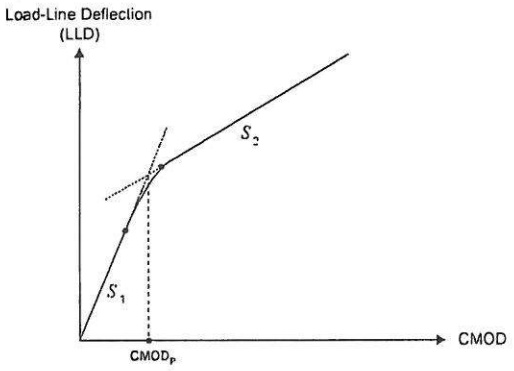

Fig. 3(b) Relationship between load-line deflection (LLD) and CMOD

3. Modeling of Concrete Fracture Behavior

3.1 Bilinear Relationship between Load-line Deflection (LLD) and Crack-mouth-opening Displacement (CMOD)

The indirect method for obtaining fracture energy, G_F, suggested by RILEM [4] requires the complete load versus load-line deflection (LLD) curve from the three-point bend beam test. It is difficult to obtain an accurate LLD due to the effect of support crushing. To obtain an accurate LLD, a special test setup was used (Fig. 1 and 2).

A relationship between CMOD and LLD was first report by Kim [5]. In Fig. 3(a), a typical load and displacement (LLD or CMOD) response was shown. Fig. 3(b) shows a typical relationship between LLD and CMOD which is bilinear in shape. The initial slope S_1 is valid in the linear elastic portion of the load versus deflection responses. Near the peak load, the slope S_1 then gradually changes to S_2 during the formation of the fracture process zone, which is the nonlinear zone in the vicinity of the crack tip. At the peak load, the fracture process zone is fully developed, and produces traction-free cracked surface after which the specimen exhibits a linear relationship between LLD and CMOD with a constant slope S_2. The values of S_1 and S_2 can be experimentally evaluated. According to previous works by other researchers [5,12], the value of S_1 and S_2 were reported to be a material property.

3.2 Determination of Fracture Energy

To derive the relationship for determining the fracture parameters from the load-CMOD response of a notched beam test (Fig.1), the following assumptions are utilized:

1. Fracture energy, G_F, is a material property. And it can be defined as the accumulation of the energy as the notched beam finally separates into two halves.
2. The fracture process zone is fully developed at the peak load, and when a crack propagates the size of fracture process zone does not change.

From the global energy balance concept, the work done by external load, F, at any instant of time Δt during the fracture process can be expressed, by using the load vs. deflection curve, as

$$F = W + U = \int_{\delta=0}^{\delta=\delta} P d\delta \qquad (1)$$

where W = total energy consumed in the fracture process zone for crack growth (plastic energy), U = elastic strain energy, P = external load acting on the beam, and $d\delta$ = incremental load-line deflection (LLD).

The fracture energy is defined as the amount of total energy absorbed during the fracture process divided by the fracture area, which can be express as

$$G_F = \frac{dF}{Bd\Delta a} = \frac{d(W+U)}{Bd\Delta a} = \frac{\int_{\delta=0}^{\delta=\infty} P d\delta}{B(D-a_0)} \qquad (2)$$

where B = width of the beam, Δa = crack growth, D = depth of the beam and a_0 = pre-notched crack length (see Fig. 4).

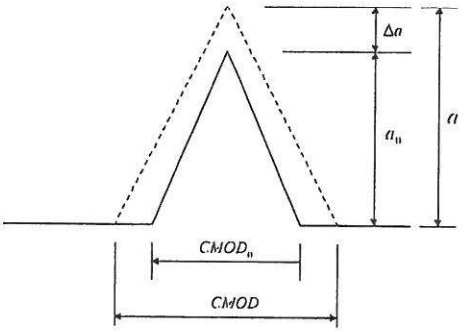

Fig. 4 Relationship between CMOD and crack propagation

The energy needed to produce a small increment of load-line deflection, dF is

$$dF = P d\delta \qquad (3)$$

From the typical three-point-bend beam test, the relationship between LLD and CMOD ($d\delta/dCMOD$) is found to be bilinear. Then substituting Eq. (2) into Eq. (3) gives

$$\left(\frac{d\delta}{dCMOD}\right)PdCMOD = G_F B d\Delta a \qquad (4)$$

By integrating Eq. (4) from time, $t = 0$ ($\Delta a = 0$), to time, $t = \Delta t$ ($\Delta a = \Delta a$) it gives the following result at any time instant, Δt, as

$$\left(\frac{d\delta}{dCMOD}\right)_1 \int_0^{CMOD_P} PdCMOD + \left(\frac{d\delta}{dCMOD}\right)_2 \int_{CMOD_P}^{CMOD} PdCMOD$$

$$= G_F B \int_{\Delta a=0}^{\Delta a=\Delta a} d\Delta a = \int_{\delta=0}^{\delta=\delta} Pd\delta \qquad (5a)$$

The first term on the left side of Eq. (5a) represents the linear elastic range of the load-CMOD curve, and the second term represents the post-peak response. In a more convenient form, the above equation can be written as

$$S_1 \int_0^{CMOD_P} PdCMOD + S_2 \int_{CMOD_P}^{CMOD} PdCMOD$$

$$= G_F B \int_{\Delta a=0}^{\Delta a=\Delta a} d\Delta a = \int_{\delta=0}^{\delta=\delta} Pd\delta \qquad (5b)$$

where S_1 is the slope of LLD-CMOD curve in the linear-elastic region, and S_2 is the slope of LLD-CMOD curve in the post-peak region (or plastic region). The region between the linear-elastic and post-peak region is approximated by extending the slope S_1 and S_2 till they intersect, as shown in Fig. 3(b). The intersection of S_1 and S_2 is represented by $CMOD_P$ in Eqs. (5a) and (5b).

To determine the fracture energy (G_F), Eq. (2) is substituted into the Eq. (5b). Then the relationship to calculate the G_F can be expressed as

$$G_F B(D - a_0) = G_F B \int_{\Delta a=0}^{\Delta a=D-a_0} d\Delta a = \int_{\delta=0}^{\delta=\infty} Pd\delta$$

$$= S_1 \int_0^{CMOD_P} PdCMOD + S_2 \int_{CMOD_P}^{\infty} PdCMOD \qquad (6)$$

Therefore the procedures for determining fracture energy (G_F) by using the load-CMOD curve can be briefly described as follows:

1. Determine the correlated constant S_1 and S_2 by relating accurately measured LLD to CMOD of the beam.
2. G_F is determined by multiplying the correlated constants (S_1 or S_2) to the corresponding area under the load-CMOD curve as shown in the Eq. (6).

3.3 Determination of Crack Growth

The phenomenon of slow crack growth prior to the peak load, caused by the growth of the fracture process zone in front of the crack tip, has long been noticed. For the LEFM based Two-Parameter Fracture Model, the critical crack length (a_c) was used to study the growth of fracture process zone [2,11]. In this study, based on the proposed nonlinear fracture model, the crack growth (Δa) at any instant of time, Δt, during the fracture process can be expressed by rearranging Eq. (5b) as

$$\Delta a = \frac{1}{G_F B} \int_0^{\delta} Pd\delta$$

$$= \frac{1}{G_F B}\left(S_1 \int_0^{CMOD_P} PdCMOD + S_2 \int_{CMOD_P}^{CMOD} PdCMOD \right) \qquad (7)$$

From Eq. (7), the crack growth (Δa) at any instant of time can be determined by using either the load vs. CMOD curve or the load vs. deflection curve. If during the interested time instant, the fracture process zone has not been fully developed, or the peak load has not been reached, the second term of the load-CMOD related equation will be zero.

Therefore the critical crack length, a_c, as defined by the Two-Parameter Fracture Model (TPFM) can be determined by using Eq. (7) to obtain Δa at the peak load as follows:

$$a_c = a_0 + \Delta a_c \qquad (8)$$

where a_0 = initial notch depth, and Δa_c = crack growth at peak load.

3.4 Determination of Fracture Resistance

During the fracture process, the material outside the fracture process zone is assumed to be linear elastic, whereas those inside the process zone behaves nonlinear and inelastic [1,9]. The fracture process zone gradually grows until reaching its full size at the peak load. After the peak load, the process zone moves upwards as the microcrack grows, but the process zone size remains unchanged unless the confinement effect is encountered. No microcracks will occur outside the process zone, thus the material outside of the process zone simply unloads elastically.

To determine the fracture parameters from the load-displacement responses of a beam test, the following assumption is used.

1. The elastic components of LLD (δ_E) and CMOD ($CMOD_E$) at any instant can be calculated by considering the material unloads and reloads elastically with the constant initial stiffness K_i of the load-displacement (δ or CMOD) curve.
2. The beam displacements either load-line deflection or CMOD can be separated into two components, the elastic component and plastic component, occurring during crack propagation. This phenomenon can be expressed as

$$\delta = \delta_E + \delta_P \tag{9a}$$

$$CMOD = CMOD_E + CMOD_P \tag{9b}$$

where δ and $CMOD$ = total load line deflection (LLD) and total CMOD respectively; δ_E and δ_P = elastic and plastic component of LLD respectively; $CMOD_E$ and $CMOD_P$ = elastic and plastic component of CMOD respectively.

Applying the concept that outside the fracture process zone the material behaves elastically along with the first assumption, the relationship between the elastic component of the displacements and the material stiffness can be expressed as

$$K_i^{\delta} = \frac{dP}{d\delta_E} \tag{10a}$$

$$K_i^{CMOD} = \frac{dP}{dCMOD_E} \tag{10b}$$

where K_i^{δ} and K_i^{CMOD} are the initial stiffness determined by the slope of the load-LLD curve and load-CMOD curve respectively.

The energy required for propagating the crack (inelastic energy) can be obtained by considering the energy balance of a beam under bending at any instant as follows:

$$W = F - U \tag{11}$$

where W = energy consumed for crack propagation: F = work done by external load (external energy) and U = elastic strain energy.

By knowing the elastic component of the displacement, the plastic energy for crack propagation can be determined by subtracting the elastic strain energy from the external work done. Therefore Eq. (11) can be expressed in terms of the load-LLD relationship as:

$$W = \int_{\delta=0}^{\delta=\delta} P d\delta_P = \int_{\delta=0}^{\delta=\delta} P d\delta - \int_{\delta=0}^{\delta=\delta} P d\delta_E \tag{12}$$

During crack growth, crack tip extension generally consumes some energy equal to W. The rate of change of W with respect to crack length (a), denoted by G_R, is termed *the fracture resistance* or *the strain energy release rate*. And, G_R can be expressed as:

$$G_R = \frac{1}{B}\frac{dW}{d\Delta a} = \frac{1}{B}\frac{d}{d\Delta a}(F - U) \tag{13}$$

where B = the width of the beam and Δa = crack growth or crack extension.
Rearranging the above equation gives

$$G_R B d\Delta a = dW = dF - dU \tag{14}$$

By integrating both sides of Eq. (14) between $t = 0$ ($\Delta a = 0$ and $\delta = 0$) and $t = \Delta t$ ($\Delta a = \Delta a$ and $\delta = \delta$), the G_R at any instant of time, Δt, can be expressed as:

$$G_R B \int_0^{\Delta a} d\Delta a = W = \int_0^{\delta} P d\delta - \int_{\delta=0}^{\delta=\delta} P d\delta_E \qquad (15)$$

By substituting the elastic component of LLD (δ_E) from Eq. (10a) into Eq. (15), this gives

$$G_R B \int_0^{\Delta a} d\Delta a = W = \int_0^{\delta} P d\delta - \int_{P(\delta=0)}^{P(\delta=\delta)} \frac{P dP}{K_i^{\delta}} \qquad (16)$$

Rearranging Eq. (16) leads to

$$G_R = \frac{1}{B\Delta a} \int_0^{\delta} P d\delta - \frac{1}{B\Delta a} \left[\frac{P^2}{2K_i^{\delta}} \right]_{P(\delta=0)}^{P(\delta=\delta)} \qquad (17)$$

where Δa is the crack growth at any time instant previously derived in Eq. (7) and K_i^{δ} is the initial stiffness determined from the slope of the load-LLD curve. Therefore, the strain energy release rate at any time instant can be determined from the load-LLD curve.

The G_R can also be derived using the load-CMOD curve. By applying the correlated constants S_1 and S_2, which are the relationship between LLD and CMOD obtained from the beam tests, G_R can be obtained, by substituting Eq. (5b) into Eq. (15), as follows:

$$G_R B \int_0^{\Delta a} d\Delta a = \left[S_1 \int_0^{CMOD_P} P dCMOD + S_2 \int_{CMOD_P}^{CMOD} P dCMOD \right] - \int_{\delta=0}^{\delta=\delta} P d\delta_E \qquad (18)$$

From the bi-linear relationship between LLD and CMOD as described in Eq. (4) through (6), the relationship between the LLD and CMOD in the elastic region can be expressed as

$$d\delta_E = S_1 dCMOD_E \qquad (19)$$

Substituting Eq. (10b) into Eq. (19) gives

$$d\delta_E = S_1 \frac{dP}{K_i^{CMOD}} \qquad (20)$$

Substituting Eq. (20) into Eq. (18) results to

$$G_R B \int_0^{\Delta a} d\Delta a = \left[S_1 \int_0^{CMOD_P} P dCMOD + S_2 \int_{CMOD_P}^{CMOD} P dCMOD \right] - S_1 \int_{P(\delta=0)}^{P(\delta=\delta)} \frac{P dP}{K_i^{CMOD}} \qquad (21)$$

and by rearranging Eq. (21),

$$G_R = \frac{1}{B\Delta a} \left[S_1 \int_0^{CMOD_P} P dCMOD + S_2 \int_{CMOD_P}^{CMOD} P dCMOD \right] - \frac{S_1}{B\Delta a} \left[\frac{P^2}{2K_i^{CMOD}} \right]_{P(\delta=0)}^{P(\delta=\delta)} \qquad (22)$$

where Δa is the crack growth at any instant of time and K_i^{CMOD} is the initial stiffness of the beam determined from the slope of the load-CMOD curve. Therefore, the strain energy release rate at any time instant can be determined from the load-CMOD curve.

A plot of energy release rate (G_R) versus crack extension (Δa) or crack length (a) is called a *Resistance Curve* or *R Curve*, which illustrates the material resistance to crack extension. The G_R value at any instant of time can be determined by applying Eq. (17) for the load-deflection response or Eq. (22) for the load-CMOD response.

At the instant of unstable crack growth, G_R is called G_C, *the critical strain energy release rate*, which is a measure of fracture toughness. For a three-point-bend beam test, G_C is equal to the value of G_R at the peak load, and can be calculated from Eqs. (21) and (22).

4. Test Results and Discussions

4.1 Results of Uniaxial Compression Tests

The concrete properties obtained are the compressive strength and modulus of elasticity. From the averaged test results, the silica fume concrete yield higher compressive strength (51 MPa) than that of the control concrete (41 MPa). The modulus of elasticity of the silica fume concrete was 37,583 MPa, and that of the control concrete was 38,192 MPa.

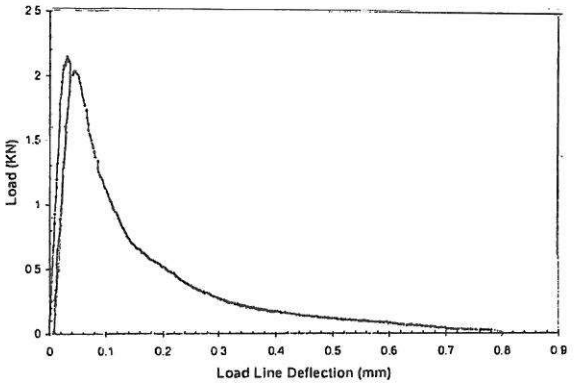

Fig. 5(a) Load vs. deflection curve for control concrete (CC)

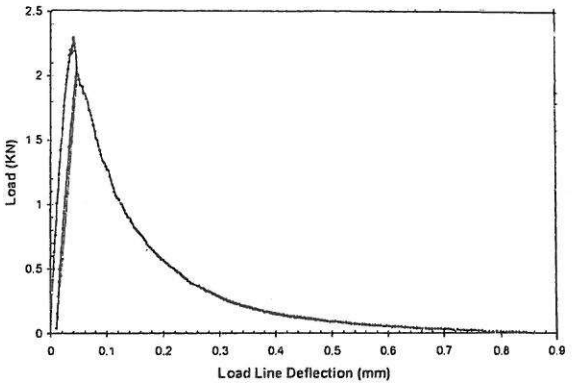

Fig. 6(a) Load vs. deflection curve for silica fume concrete (SF)

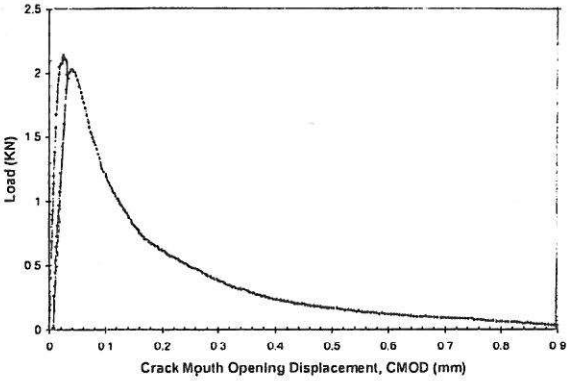

Fig. 5(b) Load vs. CMOD curve for control concrete (CC)

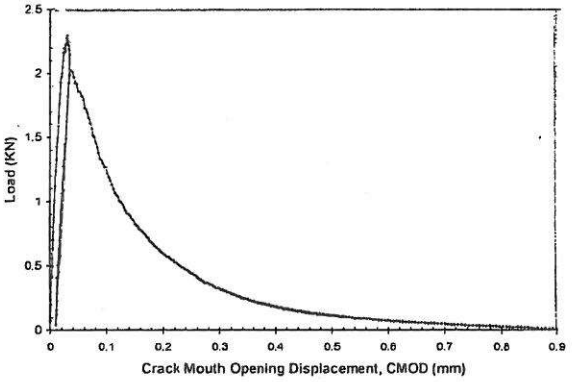

Fig. 6(b) Load vs. CMOD curve for silica fume concrete (SF)

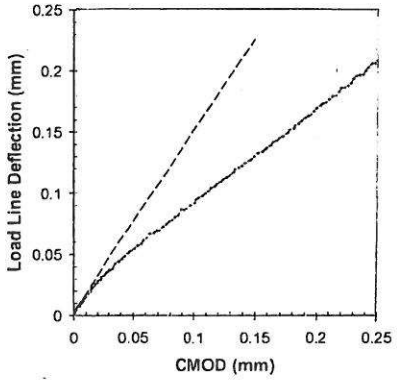

Fig. 5(c) Deflection vs. CMOD curve for control concrete (CC)

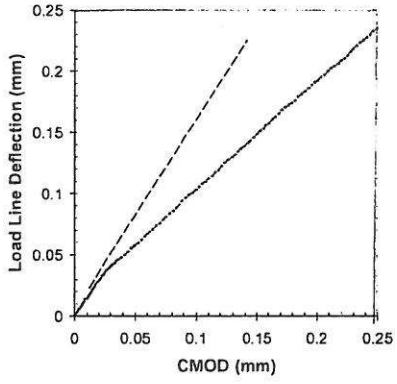

Fig. 6(c) Deflection vs. CMOD curve for silica fume concrete (SF)

Table 2 Beam test results of control concrete (CC)

Specimen Number	Peak Load	Relationship between CMOD and Deflection		Fracture Energy		Critial Energy Release Rate		Critical Crack Growth	
		S_1	S_2	CMOD Method	Deflection Method	CMOD Method	Deflection Method	CMOD Method	Deflection Method
	(KN)	(mm/mm)	(mm/mm)	(N/m)	(N/m)	(N/m)	(N/m)	(mm)	(mm)
1	2.16	1.279	0.780	82.88	83.03	45.18	42.47	7.082	6.877
2	1.98	1.284	0.829	70.88	70.76	43.65	42.64	7.537	7.119
3	2.17	1.247	0.731	76.87	76.69	44.98	45.41	8.466	8.629
Average	**2.10**	**1.270**	**0.780**	**76.88**	**76.83**	**44.60**	**43.51**	**7.695**	**7.542**

Table 3 Beam test results of silica fume concrete (SF)

Specimen Number	Peak Load	Relationship between CMOD and Deflection		Fracture Energy		Critial Energy Release Rate		Critical Crack Growth	
		S_1	S_2	CMOD Method	Deflection Method	CMOD Method	Deflection Method	CMOD Method	Deflection Method
	(KN)	(mm/mm)	(mm/mm)	(N/m)	(N/m)	(N/m)	(N/m)	(mm)	(mm)
1	2.09	1.445	0.903	89.48	87.34	58.93	55.16	9.613	9.126
2	2.29	1.446	0.883	86.54	85.86	50.89	50.20	9.414	8.845
3	2.40	1.565	0.906	96.29	94.54	56.73	53.84	10.764	10.463
Average	**2.26**	**1.486**	**0.897**	**90.77**	**89.25**	**55.52**	**53.07**	**9.931**	**9.478**

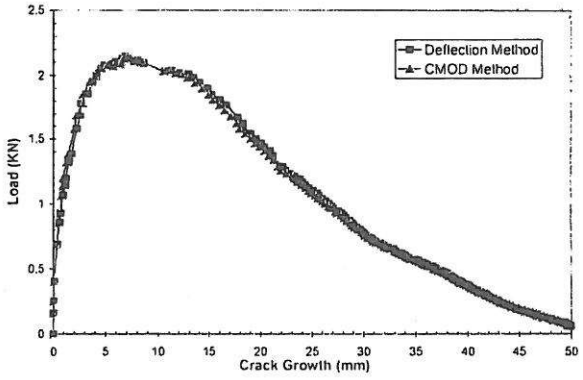

Fig. 7(a) Load vs. crack growth curve for control concrete (CC)

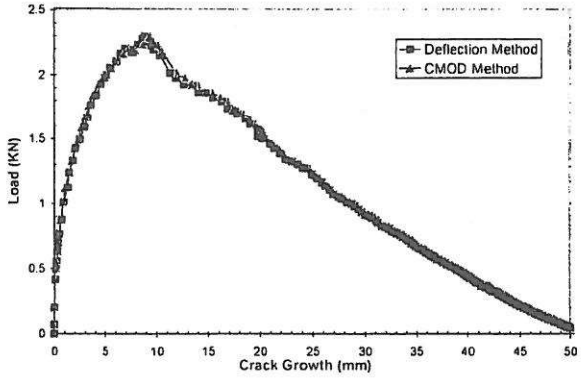

Fig. 8(a) Load vs. crack growth curve for silica fume concrete (SF)

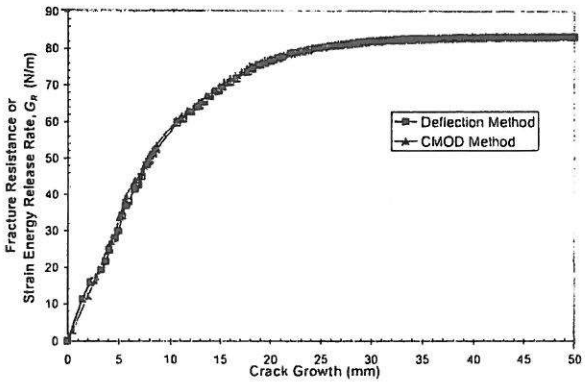

Fig. 7(b) R Curve - Control concrete (CC)

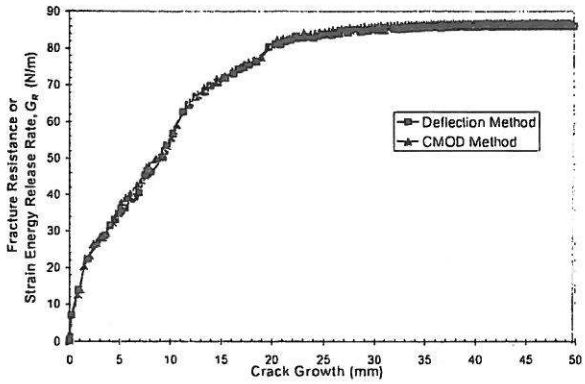

Fig. 8(b) R Curve- Silica fume concrete (SF)

4.2 Results of Bend Beam Tests Based on the Proposed Fracture Model

Typical load vs. deflection, load vs. crack-mouth-opening displacement (CMOD), and deflection vs. CMOD curves are shown in Fig. 5 and 6. Tables 2 and 3 summarize the test results obtained from the bend beam tests. CC represents the control concrete, and SF denotes silica fume concrete.

4.2.1 Bilinear Relationship between Load-Line Deflection (LLD) and CMOD

As seen in Fig. 5(c) and 6(c), a typical relationship between the deflection and CMOD is bilinear in shape, where S_1 and S_2 represent the slopes of the CMOD-deflection curve. From Tables 2 and 3, the averaged S_1 of the silica fume concrete (1.486 mm/mm) is greater than that of the control concrete (1.270 mm/mm). These differences may be attributed to the effect of the size of fracture process zone.

Since the S_1 was observed within the linear-elastic range, it is related to the elastic energy absorption. S_1 is also a result of the fracture process zone developed within the specimen configuration. A larger and softer process zone usually means a lower value of S_1. This can be reinforced by the S_1 of silica fume concrete (1.486 mm/mm) as compared to that of control concrete (1.270 mm/mm). The values of S_1 are found to agree well with those reported by other researchers [5,8,12].

As explained earlier, S_2 is the slope of the deflection and CMOD response for the post-peak softening regime. From Tables 2 and 3, silica fume concrete has the averaged S_2 of 0.897 mm/mm higher than that of the control concrete (0.780 mm/mm). Kim [5] reported the S_2 for concrete with compressive strength between 48 and 55 MPa to be 0.872 mm/mm, which is closed to the value for the silica fume concrete observed in this study. Others [8,12] reported the averaged S_2 for concrete with compressive strength about 41 MPa to be 0.790 mm/mm, which agrees well with those of the control concrete in this study.

4.2.2 Fracture Energy

In Tables 2 and 3, the values of fracture energy calculated from the load vs. CMOD curves were called the *CMOD Method*. The ones calculated from the load vs. deflection curves were called the *Deflection Method*. The results from both methods showed very good agreement. This is different from the results reported by other researchers who found discrepancy between the two concepts of determining fracture energy. With the proper test setup to overcome the support-crushing condition, and accurately measure the deflection, it will improve experimental determination of the fracture parameters.

From Tables 2 and 3 silica fume concrete had higher of the fracture energy (90.70 N/m) than that of control concrete (76.83 N/m). The results imply that fracture energy is related to compressive strength of cement composites. In addition, one may conclude that the presence of fine pozzolans such as silica fume in the cement matrix tends to improve the fracture energy of concrete.

4.2.3 Critical Energy Release Rate

Based on the proposed model, crack propagation at the crack tip consumes certain amount of energy (W), which is the plastic energy. The rate of change of W with respect to the crack growth (Δa), denoted by G_R, is termed the *fracture resistance* or the *strain energy release rate*, which can be determined from either the load vs. deflection curve or the load vs. CMOD curve. A plot between G_R and crack growth response is called the *resistance curve* or *R curve*. Typical R curves from both the load vs. CMOD response (*CMOD Method*) and the load vs. deflection response (*Deflection Method*) are shown in Fig. 7(b) and 8(b). The R curves from both methods agree well with each other due to the accurate measurement of load-line deflection.

The analytical results are summarized in Tables 2 and 3. The critical energy release rate, G_C, is defined as the value of the strain energy release rate, G_R, at the peak load. G_C is also a measure of fracture toughness. The

silica fume concrete gives the G_C of 55.48 N/m, which is higher than 44.57 N/m of the control concrete.

Replacing cement by fine pozzolans such as silica fume in the cement matrix can increase the density and reduce the thickness of the interfacial transition zone between matrix and aggregate, resulting in a stronger bond However, this can affect the fracture characteristics, and influence the brittleness behavior of concrete under loading [13,14].

4.2.4 Critical Crack Growth

The typical load-crack growth responses of concretes predicted by the proposed model are shown in Fig. 7(a) and 8(a). The load-crack growth curves based on the load vs. deflection response were called *Deflection Method*, while the ones based on the load vs. crack-mouth-opening displacement (CMOD) response were called *CMOD Method*. The results from both methods agree well with each other due to the accurate measurement of load-line deflection. The critical crack length (a_c) is defined as the summation of the initial notch depth (a_0) and the critical crack growth at peak load (Δa_c), or $a_c = a_0 + \Delta a_c$.

The proposed fracture model is derived based on elastic and inelastic parts of material response considering the fracture process zone. From Tables 2 and 3, the results contradict the suggestion by Shah [15] that there was a decrease in the critical crack length (a_c) when concrete strength increases. Silica fume concrete has a noticeably higher a_c than that of control concrete. Taking into consideration that the average size of coarse aggregate used is 3/8 inches (9.50 mm), only the silica fume concrete (SF) yields the average critical crack growth of 9.93 mm, which is more than the average size of coarse aggregate. The control concrete (CC) yields the critical crack growth of 7.70 mm.

For the silica fume concrete, due to the strong bond between cement matrix and coarse aggregate, the cracks tend to penetrate straight through the coarse aggregates rather than deflect around them. The crack straight through coarse aggregate, which is a tougher homogenous material, consumes higher energy to propagate (G_R) than the crack along the cement matrix-aggregate interface. At the moment of fracture (at peak load), the coarse aggregate releases the energy (G_R), absorbed while resisting the crack from propagating at a shorter time period resulting in a larger critical crack length (a_c).

On the other hand, for the control concrete, due to the weaker cement matrix-coarse aggregate interface, the cracks tend to deflect to the path of least resistance, which is along the interface or around the coarse aggregate particles. Since the cement matrix-coarse aggregate interface, considered to be non-homogeneous, is weaker than the coarse aggregate, the non-planar crack along the interface gradually consumes G_R, and slowly propagates during fracture, resulting in more stable crack propagation.

5. Further Research

As being realized, error in the measurement of deflection greatly affects the determination of fracture properties and various parameters. For subsequent research, the available test data and analytical results of other researchers will be compared with those determined by the proposed fracture model to further verify its validity, and also to highlight the importance of accurate measurement of deflection.

6. Conclusions

Based on the theoretical, analytical and experimental investigations of the proposed fracture model for cementitious materials, the main contributions of this work may be summarized as follows:

1. For the three-point bend tests on notched beam, by measuring deflection using a reference frame attached to the beam, the extraneous deflection can be eliminated. The proposed fracture mechanics model was developed as an alternative means to study fracture behavior and to determine fracture parameters of concrete.

2. When proper measurements of beam deflection are performed along with crack mouth opening displacement (CMOD) measurements, the bilinear relationships between deflection and CMOD in the pre-peak and post-peak regions defined as the S_1 and S_2 respectively, are found to exist. For the proposed model, S_1 and S_2 considered as material properties serve as the important factors to relate the CMOD to the fracture parameters.
3. For the proposed fracture model, the fracture behavior such as crack growth and resistance curve can be determined without applying the finite element model. Conventional fracture parameters (e.g. critical crack growth and fracture toughness) can be determined without performing the complicated unloading-reloading during beam test as required by the Two-Parameter Fracture Model.
4. Replacing cement by fine pozzolans in cement matrix can improve the pre-peak fracture behavior of concrete e.g. the compressive strength and critical energy release rate (G_C), but does not necessarily enhance the overall fracture behavior.
5. For the three-point bend tests on notched beams, the use of the proposed fracture model with the load-CMOD relationship, could lead to a new testing standard for determining the fracture properties of cementitious materials.

Acknowledgments

The author would like to thank Professor Methi Wecharatana for his guidance and fruitful discussions. The support of the New Jersey Institute of Technology is gratefully appreciated.

References

[1] A. Hillerborg, M. Modeer, P.E. Petersson, Analysis of crack formation and crack growth in concrete by means of fracture mechanics and finite elements, Cement and Concrete Research. 6 (6) (1976) 773- 782.

[2] Y. S. Jenq, S. P. Shah, Two parameter fracture model for concrete, ASCE Journal of Structural Engineering. 112 (1) (1985) 19-34.

[3] Z. P. Bazant, B. H. Oh, Crack band theory for fracture of concrete, Materials and Structures. 16 (93) (1988) 155-177.

[4] RILEM, TC50-FMC Fracture Mechanics of Concrete, Determination of fracture energy of mortar and concrete by means of three-point bend tests on notched beams, Materials and Structures. 18 (1985) 285-296.

[5] S. K. Kim, The constant fracture angle model for cementitious materials", Ph.D. Dissertation, New Jersey Institute of Technology, New Jersey, USA, 1996.

[6] RILEM, TC89-FMT Fracture Mechanics of Concrete Test Methods, Determination of fracture parameters (K^s_{IC} and $CTOD_C$) of plain concrete using three-point bend tests, Materials and Structures. 23 (1990) 457-460.

[7] V.S. Gopalaratnam, B. S. Ye, Numerical characterization of the nonlinear fracture process in concrete, Engineering Fracture Mechanics. 40 (6) (1991) 991-1006.

[8] R. Navalurkar, C.T. T. Hsu, S. K. Kim, M. Wecharatana, True fracture energy of concrete, ACI Materials Journal. 96 (2) (1999) 213-225.

[9] P. E. Petersson, Crack growth and development of fracture zones in plain concrete and similar materials, Report TVBM-1008, Division of Building Materials, Lund Institute of Technology, Lund, Sweden, 1981.

[10] ASTM, Concrete and Mineral Aggregate, Annual Book of ASTM Standards, Section 4, Vol. 04.02, American Society for Testing and Materials, Philadelphia, 2002.

[11] Y. S. Jenq, S. P. Shah, A fracture toughness criterion for concrete, Engineering Fracture Mechanics. 21 (5) (1985) 1055-1069.

[12] R. Navalurkar, Fracture mechanics of high strength concrete members, Ph.D. Dissertation, New Jersey Institute of Technology, New Jersey, USA, 1996.

[13] A. Goldman, A. Bentur, Bond effects in high-strength silica fume concrete, ACI Materials Journal. 86 (5) (1989) 440-447.

[14] A. M. Rosenberg, M. Arnold, J. M.Gaidis, New mineral admixture for high strength concrete, Concrete International. 11 (4) (1989) 31-36.

[15] S. P. Shah, Fracture toughness of high-strength concrete, ACI Materials Journal. 87 (3) (1990) 260-265.